Pinch point singularities of tensor spin liquids

Pinch point singularities of tensor spin liquids

Abhinav Prem,[1,*] Sagar Vijay,[2] Yang-Zhi Chou,[1] Michael Pretko,[1] and Rahul M. Nandkishore[1]
[1]*Department of Physics and Center for Theory of Quantum Matter, University of Colorado, Boulder, Colorado 80309, USA*
[2]*Department of Physics, Massachusetts Institute of Technology, Cambridge, Massachusetts 02139, USA*

(Received 17 July 2018; revised manuscript received 17 September 2018; published 26 October 2018)

Recently, a new class of three-dimensional spin liquid models have been theoretically discovered, which feature generalized Coulomb phases of emergent symmetric tensor $U(1)$ gauge theories. These "higher rank" tensor models are particularly intriguing due to the presence of quasiparticles with restricted mobility, such as fractons. We investigate universal experimental signatures of tensor Coulomb phases. Most notably, we show that tensor Coulomb spin liquids (both quantum and classical) feature characteristic pinch point singularities in their spin-spin correlation functions, accessible via neutron scattering, which can be readily distinguished from pinch points in conventional $U(1)$ spin liquids. These pinch points can thus serve as a crisp experimental diagnostic for such phases. We also tabulate the low-temperature heat capacity of various tensor Coulomb phases, which serves as a useful additional diagnostic in certain cases.

DOI: 10.1103/PhysRevB.98.165140

I. INTRODUCTION

Quantum spin liquids describe exotic, interacting spin systems, in which quantum fluctuations prevent conventional magnetic ordering all the way down to zero temperature. These phases are characterized by a pattern of long-range quantum entanglement in their ground states and the presence of exotic fractionalized excitations. Spin liquids are believed to occur in gapped and gapless varieties [1–6], and are theoretically well described as emergent gauge theories [7,8].

The gauge theory description of a spin liquid can take a number of different forms, ranging from intricate string-net models [9] to familiar $U(1)$ Maxwell theory. The latter case has a number of promising experimental candidates in the form of the "spin-ice" pyrochlore materials, including the classical spin ices $Dy_2Ti_2O_7$ and $Ho_2Ti_2O_7$, as well as the quantum spin ices $Yb_2Ti_2O_7$ and $Pr_2Zr_2O_7$ [7,10–16]. Over a range of low temperatures, these materials exist in a symmetry-preserving phase consistent with the expected behavior of a deconfined Coulomb phase of an emergent $U(1)$ gauge field. It is possible that in some materials, this emergent electromagnetism may survive down to zero temperature, providing an example of a $U(1)$ quantum spin liquid. Regardless, we may conclusively identify these materials as having at least classical spin liquid behavior: resisting symmetry breaking down to unusually low temperatures due to frustration between many energetically equivalent classical configurations.

Conventional $U(1)$ spin liquids exhibits striking experimental signatures. Most notably, the Coulomb phase of a $U(1)$ gauge theory exhibits characteristic "pinch point" singularities in its correlation functions; these pinch points may be observed in spin-spin correlation functions that are readily measured via neutron scattering experiments, which have been usefully applied to numerous spin liquid candidates [3,17–21]. In the quantum spin liquid, these singularities arise as a direct consequence of the gapless excitations of the system, corresponding to the emergent photon of the $U(1)$ gauge theory. Such singularities are absent in gapped quantum spin liquids.

The conventional $U(1)$ spin liquid, described in terms of an emergent Maxwell theory, has been a subject of intense theoretical and experimental study during the past two decades. We refer the reader to some reviews for an initial overview [7,18], and to some selected literature for further details [8,10,11,17,19,22–37]. Meanwhile, recent theoretical developments have uncovered a new class of generalized $U(1)$ spin liquids which we have only just begun to understand [38–41]. Instead of the familiar vector $U(1)$ gauge field of Maxwell theory, these three-dimensional spin systems are described by the deconfined "Coulomb" phase of emergent symmetric *tensor* $U(1)$ gauge fields. Just like their vector gauge theory counterparts, such symmetric tensor $U(1)$ gauge theories have instanton instabilities in two spatial dimensions arising from issues of compactness, but have stable deconfined phases in three dimensions (except in certain special cases) [39–41].[1]

This new class of spin liquids has some properties in common with the conventional $U(1)$ spin liquid, such as protected gapless gauge modes. What sets these new tensor gauge theories apart, however, is the behavior of the emergent, gapped charge excitations, which have severe restrictions on their mobility. The gauge charges can be restricted to motion within one- or two-dimensional subspaces, or in certain models, can be restricted from moving at all. These immobile, charged excitations (termed "fractons"), as well as the gapped excitations with reduced mobility, were first obtained in completely *gapped* three-dimensional systems with intricate patterns of long-ranged entanglement, and have since been encountered in a wide variety of physical systems. We refer the reader to

*Present address: Princeton Center for Theoretical Science, Princeton University, Princeton, New Jersey 08544, USA.

[1]Compact *antisymmetric* $U(1)$ tensor gauge fields tend to not have deconfined phases in three or fewer dimensions [42–46].

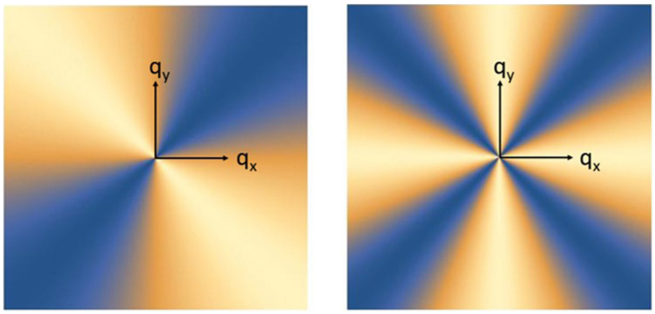

FIG. 1. The pinch point singularities of a conventional $U(1)$ spin liquid (left) have a characteristic twofold symmetry. In contrast, pinch points of the rank-2 tensor spin liquids (right) have a characteristic fourfold symmetry, which should allow for easy distinction in neutron-scattering data. [The two plots display $\langle E^x(q)E^y(-q)\rangle$ (left) and $\langle E^{xx}(q)E^{yy}(-q)\rangle$ (right), with cross sections taken in the $q_z = 0$ plane.]

a recent review [47] for an overview of fractons, and to the literature for further details [48–88]. Gapped fracton phases, such as Haah's code or the X-cube model, display glassy quantum dynamics in their approach to equilibrium, which may serve as a useful diagnostic of these systems [57]. On the other hand, the "generalized" Hall conductivity predicted for the two-dimensional chiral gapped tensor gauge theory [56] has been conjectured to be a manifestation of the torsional Hall viscosity [77], providing another experimental signature of fracton physics.

While the gapless tensor $U(1)$ spin liquids have likewise been a topic of intense recent theoretical study, little is known about sharp experimental signatures of these systems. In the present work we will identify certain key signatures which can be used to diagnose the presence of different types of emergent tensor $U(1)$ spin liquids in experiments, placing particular emphasis on the rank-2 spin liquids, i.e., where the emergent gauge field in the system of interest is a two-component symmetric tensor. Such experimental metrics may provide important clues which guide the search for physical systems realizing tensor Coulomb behavior.

Most notably, we study the behavior of the spin-spin correlation functions of these new spin liquids. We begin by studying the ground state correlation functions of the quantum version of these spin liquids by making use of their low-energy effective field theory [39–41]. We show that the spin-spin correlation functions exhibit a new pinch point singularity due to the tensor nature of the gapless gauge excitations. Certain features of these singularities are universal, independent of details at the lattice scale, and are applicable to any microscopic model featuring a tensor Coulomb phase. These universal features allow the tensor $U(1)$ spin liquids to be easily distinguished from a conventional $U(1)$ spin liquid in experiment. For rank-2 tensor models, we show that the pinch points have a characteristic *fourfold* symmetry, as opposed to the twofold symmetry of pinch points in more conventional spin liquids (see Fig. 1), which will allow for straightforward detection in experiments. We note that the singularities generically remain pointlike in these systems, in contrast with the "pinch line" singularities seen in certain nongeneric tensor spin liquid models [89]. We then move on to study the finite-temperature spin-spin correlation functions of classical tensor Coulomb spin liquids, which we show have similar pinch point singularities. These pinch points, both classical and quantum, can be directly accessed via neutron scattering data. The scattering function for neutrons impinging on the sample is given directly in terms of the spin-spin correlation functions of the system, which can thereby be effectively mapped out in order to see pinch point singularities [3,18–21]. The detection of such fourfold pinch points would be an important confirmation of an emergent tensor gauge structure, and therefore of fracton behavior. Such an experimental detection of fractons would be of broad interest to the numerous research communities studying these particles, ranging from quantum information to many-body localization [47].

In addition to pinch point singularities, we also tabulate the heat capacities of the various tensor $U(1)$ spin liquids, which should be readily accessible to experiments. The gapless modes of these models lead to a power-law contribution to the heat capacity, distinguishable from that of vector $U(1)$ models in certain cases. In a conventional $U(1)$ spin liquid, the linear dispersion of the gauge modes means that their contribution to the heat capacity cannot be easily separated from that of phonons, and hence does not serve as a useful experimental probe. In contrast, some of the tensor $U(1)$ spin liquids have nonlinearly dispersing gauge modes which provide a dominant contribution to the low-temperature heat capacity and should thus serves as a useful diagnostic for the tensorial nature of the gauge field.

II. REVIEW OF TENSOR GAUGE THEORY

We here review the basic properties of the two simplest tensor $U(1)$ quantum spin liquids and refer the reader to previous literature [39–41] for more details. These spin liquids are described in terms of an emergent, symmetric rank-2 tensor field A_{ij}, where all indices refer to spatial coordinates $i, j = 1, 2, 3$. This gauge field possesses a canonical conjugate variable E_{ij}, which corresponds to a generalized electric field. As we discuss below, there is a direct microscopic mapping from certain quantum rotor models (equivalent to large-S spin models) onto such tensor gauge theories, with the gauge invariant observables, such as electric field, directly corresponding to spin variables. Multiple such tensor gauge theories may be defined, each of which is uniquely determined by different chosen forms for Gauss's law.

A. Scalar charge theory

One simple theory we can write down has a Gauss's law of the form

$$\partial_i \partial_j E^{ij} = \rho, \tag{1}$$

for a scalar-valued charge ρ. (We use the Einstein summation convention throughout, with repeated indices summed over.) Within the low-energy sector, the corresponding gauge transformation is

$$A_{ij} \rightarrow A_{ij} + \partial_i \partial_j \alpha, \tag{2}$$

where α is a scalar function with arbitrary spatial dependence. This system admits gapless gauge modes, with a low-energy

Hamiltonian given by

$$H = \int d^3x \frac{1}{2}(E^{ij}E_{ij} + B^{ij}B_{ij}), \tag{3}$$

where $B^{ij} = \epsilon^{iab}\partial_a A_b^j$ is the gauge-invariant magnetic field operator. This Hamiltonian leads to five gapless gauge modes, each with a linear dispersion $\omega \propto q$. The existence of five gauge modes can be understood via a simple counting argument. A symmetric tensor in three dimensions has six independent degrees of freedom. The scalar charge represents a single gapped degree of freedom, which leaves five degrees of freedom for the gapless gauge modes, as discussed in Refs. [39–41].

Much more notable than the gauge mode, however, is the charge sector of the theory, which has properties with no analog in more conventional gauge theories. In addition to the conservation of charge

$$\int d^3x\, \rho = \text{const}, \tag{4}$$

this theory also exhibits conservation of dipole moment

$$\int d^3x\, (\rho x^i) = \text{const}. \tag{5}$$

This conservation law has the severe immediate consequence that the fundamental charges of the theory are strictly immobile, i.e., are fracton excitations. Only charge-neutral bound states, such as dipolar bound states, are free to move around the system.

B. Vector charge theory

It is also possible to consider a slightly modified theory of a rank-2 tensor, with a different version of Gauss's law, which takes the form

$$\partial_i E^{ij} = \rho^j, \tag{6}$$

for a vector-valued charge density ρ^j. The corresponding low-energy gauge transformation is

$$A_{ij} \to A_{ij} + \partial_i\alpha_j + \partial_j\alpha_i, \tag{7}$$

where α_i is a function with arbitrary spatial dependence. The low-energy Hamiltonian for the gauge sector of this theory takes the same form as in Eq. (3), but with a modified magnetic field operator $B^{ij} = \epsilon^{iab}\epsilon^{jcd}\partial_a\partial_c A_{bd}$. In this case, the Hamiltonian leads to three gapless quadratically dispersing gauge modes $\omega \propto q^2$. This theory also possesses an unusual set of charge conservation laws, in that the vector charges obey not only conservation of charge,

$$\int d^3x\, \rho^i = \text{const}, \tag{8}$$

but also a second conservation law pertaining to the angular moment of charge,

$$\int d^3x\, \epsilon^{ijk}\rho_j x_k = \text{const}. \tag{9}$$

This second conservation law has the unusual consequence that the vector charges are restricted to motion only in the direction of their charge vector, while motion in the perpendicular directions is ruled out by gauge invariance. This causes the charges to behave like one-dimensional particles, despite being embedded in three-dimensional space.

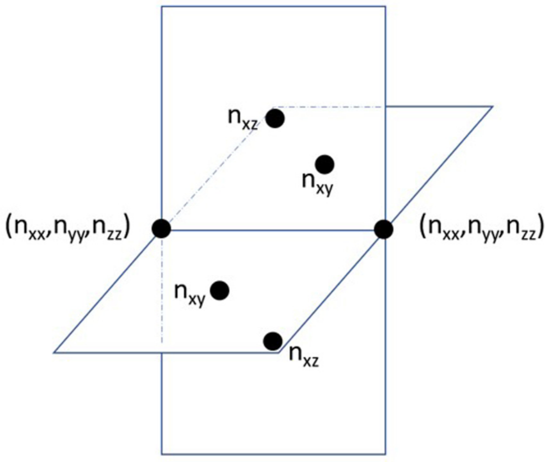

FIG. 2. A microscopic model for the tensor gauge theories can be easily obtained via quantum rotors, with one quantum rotor on each plaquette of a cubic lattice, and three rotors on each site.

C. Microscopic models

We here review some microscopic models, first discussed in Ref. [38], which naturally give rise to the two theories discussed above. These theories can be realized in the context of lattice quantum rotor systems, which has a Hilbert space equivalent to that of a large-S spin system. In fact, both the scalar and vector charge theories can be realized with the same microscopic Hilbert space, with different choices of Hamiltonian. We here focus on the vector charge theory, which is slightly simpler to construct. We refer the reader to Refs. [38,39] for more details.

The Hilbert space can be constructed by placing quantum rotors on the vertices and plaquettes of a cubic lattice, with each rotor label by its integer angular momentum quantum number, which we write as n (Fig. 2). Specifically, we place one rotor on each plaquette, which we label as n_{xy}, n_{xz}, or n_{yz}, according to which plane that plaquette is a part of. We place three rotors on each vertex, which we label as (n_{xx}, n_{yy}, n_{zz}). This choice of labeling is suggestive, since it shows that the rotors have been placed in such a way that the components can transform into each other in a tensorial way under spatial rotations.

We must now write down a Hamiltonian in such a way as to mimic the desired Gauss's law. For the case of the vector charge theory, the low-energy (i.e., charge-free) Gauss's law constraint is just $\partial_i E^{ij} = 0$. One can naturally regularize this equation on the cubic lattice by letting the constraint live on links, taking sums and differences of all the electric tensor components adjacent to that link. We can begin to mimic this in rotor language by writing down a term in the Hamiltonian of the form

$$H_0 = V \sum_{\text{links}} \left(\sum_{\text{adj}} n \right)^2, \tag{10}$$

where the outer sum runs over all links of the lattice. The inner sum runs over all rotors adjacent to that link, which importantly must also share an index in common with its direction. For example, for an x directed link, the sum will include n_{xx}, n_{xy}, and n_{xz} terms. As a technical detail, we note that vertex variables must actually be counted *twice* in this sum, as compared to the plaquette variables, for reasons discussed in Ref. [38]. Note that the form of the Hamiltonian seen above counts all of the n with positive signs. In order to obtain the correct behavior of the Gauss's law, one must therefore stagger the signs in mapping from n to E. In other words, we can write $E_{xx} = \eta\, n_{xx}$, where η alternates positive and negative from one site to the next, and similarly for all other components.

The Hamiltonian above already captures the Gauss's law constraint, which we will see is the most important piece for understanding the pinch point singularities, to be discussed next. For a classical spin liquid, at finite temperature, imposing this constraint is sufficient to extract all of the relevant physics. For a quantum spin liquid, however, one must add additional terms to the rotor Hamiltonian in order to mimic the $E^2 + B^2$ behavior of the tensor Maxwell Hamiltonians described above. These terms can be added in straightforward fashion. We refer the reader to Refs. [38,39] for more details.

III. PINCH POINT SINGULARITIES

We have seen that the physical spin operators of a spin liquid can be mapped directly onto gauge-invariant field operators of an emergent gauge theory. We here focus on the case where the spins map onto electric field operators (similar arguments apply when the spins are mapped onto magnetic operators.). We calculate the correlation function of a rank-2 electric tensor as

$$\langle E_{ij}(x)E_{k\ell}(0)\rangle \tag{11}$$

and similarly for tensors of higher rank. The physical spin correlators in the long distance limit will be dominated by the correlation functions of the gapless gauge field, and given by some linear combination of these tensor correlation functions

$$\langle S_z(x)S_z(0)\rangle = C^{ijk\ell}\langle E_{ij}(x)E_{k\ell}(0)\rangle. \tag{12}$$

Here the separation x is implicitly large, and the structure factor $C^{ijk\ell}$ is constrained by the symmetries of the underlying lattice. In the following, we focus on the universal (long distance, small wave vector) behavior of these correlation functions, which should not depend on the precise form of the structure factors.

A. Conventional $U(1)$ spin liquid

For convenience, we recall the calculation of pinch point singularities in a conventional $U(1)$ spin liquid, which will generalize naturally to the tensor case. The appropriate low-energy Hamiltonian takes the usual Maxwell form,

$$H = \int d^3x \frac{1}{2}(E^iE_i + B^iB_i), \tag{13}$$

where $B^i = \epsilon^{ijk}\partial_j A_k$, and we implicitly have the gauge constraint $\partial_i E^i = 0$. In momentum space, the Hamiltonian decouples into independent harmonic oscillator modes, and thus by equipartition, the two terms of the Hamiltonian contribute equally to the ground state energy. For Maxwell theory, the dispersion is linear $\omega \propto q$, leading to a zero point energy proportional to q for each mode, from which we conclude that

$$\langle E^i(q)E_i(-q)\rangle \propto q. \tag{14}$$

We must now restore the full tensor structure. To do this, we start with the isotropic result δ^{ij}, as if all modes were present, and then project out the divergence mode, which is absent from the low-energy sector. The final electric field correlator then takes the form

$$\langle E^i(q)E^j(-q)\rangle \propto q\left(\delta^{ij} - \frac{q^iq^j}{q^2}\right). \tag{15}$$

The second term, arising due to the projection into the gauge sector, leads to "pinch point" singularities in the correlation function, in that the ratio q^iq^j/q^2 has different limits upon approaching the origin $\mathbf{q} = 0$ from different directions, as depicted schematically in Fig. 1. These singularities can be easily detected via neutron scattering, thereby serving as a powerful tool for diagnosing $U(1)$ spin liquids in experiments. We note that an important feature of the correlation function Eq. (15) is its twofold symmetry, illustrated explicitly in, e.g., the $\langle E^x(q)E^y(-q)\rangle$ correlator shown in Fig. 1.

One can also consider the finite-temperature behavior of correlation functions in a classical $U(1)$ spin liquid, where the quantum splitting of degeneracies is unimportant. In this case, we impose the spin-ice constraint $\partial_i E^i = 0$, but regard all states within this spin-ice manifold as being roughly energetically equivalent. The free energy of the system is then set almost entirely by entropic effects $F \approx -TS$. By the central limit theorem, the probability distribution for the emergent electric field E^i must be Gaussian in the thermodynamic limit [18], such that

$$F/T = K\int d^3x\, E^iE_i, \tag{16}$$

for some constant K, where the spin-ice constraint $\partial_i E^i = 0$ is left implicit. Were it not for this constraint, we could simply conclude that $\langle E_i(q)E_j(-q)\rangle \propto (1/K)\delta_{ij}$. After projecting out the longitudinal component, however, the correct correlation function behaves as

$$\langle E_i(q)E_j(-q)\rangle_c \propto \frac{1}{K}\left(\delta_{ij} - \frac{q_iq_j}{q^2}\right), \tag{17}$$

where the subscript c denotes "classical," indicating a simple thermal correlation function. Note that this classical correlation function has the same singular tensor structure as the quantum case, but with a different prefactor. Note also that the pinch point structure comes purely from projection into the spin-ice manifold, such that the basic result is independent of the specific model (16) used to derive it.

B. Scalar charge theory

For the scalar charge theory, defined by the Gauss's law $\partial_i\partial_j E^{ij} = \rho$, the low-energy Hamiltonian takes the same schematic form as in Maxwell theory, as seen in Eq. (3), with the implicit gauge constraint $\partial_i\partial_j E^{ij} = 0$. As in Maxwell theory, the dispersion of the gauge modes is linear. By the same equipartition argument as before, the zero-temperature quantum correlation function satisfies

$$\langle E^{ij}(q)E_{ij}(-q)\rangle \propto q. \tag{18}$$

To get the correct tensor structure, we start with the isotropic symmetric tensor $\frac{1}{2}(\delta^{ik}\delta^{j\ell}+\delta^{i\ell}\delta^{jk})$ and project out the q^iq^j component

$$\langle E^{ij}(q)E^{k\ell}(-q)\rangle \propto q\left(\frac{1}{2}(\delta^{ik}\delta^{j\ell}+\delta^{i\ell}\delta^{jk})-\frac{q^iq^jq^kq^\ell}{q^4}\right), \tag{19}$$

which exhibits a pinch point singularity at $q=0$, in the sense of different limiting behavior when approaching the origin from different directions. Notice, however, that the rank-4 tensor structure of the correlation function (19) manifests itself in a characteristic *fourfold* singularity pattern, as opposed to the twofold symmetry of pinch points in a conventional $U(1)$ spin liquid. Note also that the fourfold symmetry is present only in certain components of this rank-4 tensor, e.g., $\langle E^{xx}E^{yy}\rangle$, while others such as $\langle E^{xx}E^{xx}\rangle$ only possess a twofold symmetry. However, the presence of a fourfold symmetry in certain components of the correlator, as depicted in Fig. 1, will allow for easy distinction between this tensor gauge theory and more familiar spin-ice models described by vector gauge theories. Importantly, note that this fourfold symmetry only holds in the immediate vicinity of the pinch point singularity, while the overall symmetry of the spin-spin correlation functions throughout the Brillouin zone is determined by the symmetry of the underlying lattice.

In close analogy with the conventional $U(1)$ spin liquid, we can also consider a classical analog of this tensor Coulomb phase, where only the spin-ice constraint $\partial_i\partial_jE^{ij}=0$ is important, while the quantum splitting of degeneracies can be ignored. By the central limit theorem, we can once again conclude that the probability distribution for E_{ij} takes a Gaussian form, such that the free energy can be written as

$$F/T = K\int d^3x\, E^{ij}E_{ij}, \tag{20}$$

for some constant K. The classical correlation function then takes the form

$$\langle E^{ij}(q)E^{k\ell}(-q)\rangle_c \propto \frac{1}{K}\left(\frac{1}{2}(\delta^{ik}\delta^{j\ell}+\delta^{i\ell}\delta^{jk})-\frac{q^iq^jq^kq^\ell}{q^4}\right), \tag{21}$$

which has the same fourfold behavior as the quantum correlation function (19), but with a different, nonuniversal prefactor. Again, the pinch point structure comes purely from projection into the "higher rank" spin-ice manifold.

C. Vector charge theory

For the vector charge theory, defined by $\partial_iE^{ij}=\rho^j$, the low-energy Hamiltonian leads to gapless gauge modes with *quadratic* dispersion $\omega\sim q^2$, unlike the previously studied theories. The implicit gauge constraint in the low-energy sector is now $\partial_iE^{ij}=0$. By the usual equipartition argument, the zero-temperature quantum correlation function satisfies

$$\langle E^{ij}(q)E_{ij}(-q)\rangle \propto q^2. \tag{22}$$

In order to restore the tensor structure, we can start with the isotropic symmetric tensor then add terms to project off components along the q direction,

$$\langle E^{ij}(q)E^{k\ell}(-q)\rangle \propto q^2\left[\frac{1}{2}(\delta^{ik}\delta^{j\ell}+\delta^{i\ell}\delta^{jk})+\frac{q^iq^jq^kq^\ell}{q^4}-\frac{1}{2}\left(\delta^{ik}\frac{q^jq^\ell}{q^2}+\delta^{jk}\frac{q^iq^\ell}{q^2}+\delta^{i\ell}\frac{q^jq^k}{q^2}+\delta^{j\ell}\frac{q^iq^k}{q^2}\right)\right]. \tag{23}$$

It can be readily checked that this expression annihilates any rank-2 tensor with a component along q in either index. This correlation function once again has a pinch point singularity at $q=0$ with a characteristic fourfold symmetry, similar to that of the scalar charge theory. However, the pinch point singularity of the vector charge theory has a different power-law behavior than that of either the conventional $U(1)$ spin liquid or the scalar charge theory. The exponent with which this correlator diverges can thus be readily identified in neutron scattering data, making this type of spin liquid particularly simple to distinguish in experiments.

In close analogy with the previous section, we can also immediately write down the finite-temperature correlation function of the corresponding classical tensor Coulomb phase as

$$\langle E^{ij}(q)E^{k\ell}(-q)\rangle \propto \frac{1}{K}\left[\frac{1}{2}(\delta^{ik}\delta^{j\ell}+\delta^{i\ell}\delta^{jk})+\frac{q^iq^jq^kq^\ell}{q^4}-\frac{1}{2}\left(\delta^{ik}\frac{q^jq^\ell}{q^2}+\delta^{jk}\frac{q^iq^\ell}{q^2}+\delta^{i\ell}\frac{q^jq^k}{q^2}+\delta^{j\ell}\frac{q^iq^k}{q^2}\right)\right], \tag{24}$$

which has the same fourfold symmetry as the quantum case (15).

D. Traceless theories

For completeness, we briefly discuss the pinch point singularities of the traceless versions of the rank-2 gauge theories, which will display the same fourfold symmetry pattern. When the scalar charge theory is given an extra tracelessness constraint $E^i_i=0$, its dispersion remains linear, and the corresponding pinch points have the same scaling $\langle E^{ij}(q)E^{k\ell}(-q)\rangle\propto q$, so this theory is not easily distinguished from its traceful cousin via neutron scattering. In contrast, when the vector charge theory has tracelessness imposed, its dispersion becomes cubic $\omega\propto q^3$. In this case, the scaling of the pinch point singularities changes to $\langle E^{ij}(q)E^{k\ell}(-q)\rangle\propto q^3$, which can be clearly distinguished in experiments from all of the previously studied $U(1)$ spin liquids.

TABLE I. Summary of heat capacities for the rank-2 tensor $U(1)$ spin liquids.

Theory	Gauge dispersion	Polarizations	Heat capacity
Scalar charge	$\omega \sim q$	5	$C \sim T^3$
Traceless scalar charge	$\omega \sim q$	4	$C \sim T^3$
Vector charge	$\omega \sim q^2$	3	$C \sim T^{3/2}$
Traceless vector charge	$\omega \sim q^3$	2	$C \sim T$

IV. HEAT CAPACITY

Besides the ground state correlation functions, another useful diagnostic for certain tensor Coulomb spin liquids is the low-temperature heat capacity. Since all the emergent charges are gapped excitations, their contribution to heat capacity will be exponentially suppressed, i.e., follow Arrhenius behavior, as discussed in Ref. [57]. Hence, the low-temperature heat capacity will be dominated by the contribution from the gapless gauge modes, which depends on both the number of gauge modes and their dispersion.

Let us assume that the gauge mode has n_p independent polarizations and that its dispersion is given by $\omega \sim q^a$. Then the energy density at temperature T is given by

$$E/V \sim n_p \int d^3q \, \frac{q^a}{e^{q^a/T} - 1} = \frac{4\pi n_p}{a} \Gamma\left(\frac{3+a}{a}\right) \zeta\left(\frac{3+a}{a}\right) T^{\frac{3+a}{a}}, \tag{25}$$

where we have set $k_B = 1$. For the usual Maxwell theory in 3+1D, where $a = 1$ and $n_p = 2$, this reproduces the usual heat capacity

$$C_v/V = \frac{d}{dT}(E/V) = \frac{8\pi^5 T^3}{15}, \tag{26}$$

in units where the speed of light $c = 1$.

For the tensor $U(1)$ spin liquids, the results are tabulated in Table I. For both the traceful and traceless versions of the scalar charge theory $C_v \sim T^3$, which is indistinguishable from the usual Maxwell theory (and from phonon contributions) since only the numerical prefactors are different between these, reflecting the difference in the number of independent gauge modes. In principle, one can imagine detecting the number of gauge modes in the system by deforming it along different directions by applying stress/strain, which will result in the gauge modes along that direction gaining a different dispersion. However, both the traceful and traceless versions of the vector charge theory display markedly different temperature scaling, which should serve as clear and distinctive experimental signature of these phases.

V. CONCLUSIONS

In this work we have identified several key signatures which can be used to diagnose tensor Coulomb spin liquid phases, which feature an emergent deconfined $U(1)$ symmetric tensor gauge theory. Most notably, these phases exhibit pinch point singularities in spin-spin correlation functions, which can be easily observed in neutron scattering data. These pinch point singularities are qualitatively different from those of a conventional $U(1)$ spin liquid, which will allow these systems to easily be distinguished from more familiar spin-ice materials. Specifically, a rank-2 tensor model has a characteristic fourfold symmetry pattern, in contrast with the twofold symmetry of pinch points in conventional $U(1)$ spin liquids. For tensor $U(1)$ spin liquids with rank higher than two, similar logic indicates that the pinch point singularity structure is determined by the properties of the low-energy gauge modes. For a rank n theory, the resulting pinch point will have a $2n$-fold symmetry.

Additionally, we tabulated the heat capacity of various tensor Coulomb spin liquids, which provides an additional metric for diagnosing certain types of these phases. These signatures may serve to inform the future search for material realizations of tensor Coulomb spin liquids. Apart from the diagnostics considered in this work, there remain several other features of tensor gauge theories which are expected to display behavior distinct from that of conventional vector gauge theories. For instance, the linear response coefficients of a tensor gauge theory should provide another useful experimental metric for establishing the presence of a tensor Coulomb phase, as should the dynamical behavior of the spin correlations (for usual vector gauge theories, this was discussed in Refs. [90,91]). These additional signatures will be discussed at length elsewhere [92].

ACKNOWLEDGMENTS

We acknowledge useful conversations and correspondence with T. Senthil, Mike Hermele, Han Ma, Leo Radzihovsky, and Han Yan. This work is partially supported by the DOE Office of Basic Energy Sciences, Division of Materials Sciences and Engineering under Award de-sc0010526 (S.V.); by NSF Grant No. 1734006 (M.P.); by a Simons Investigator Award to Leo Radzihovsky (M.P. and Y.-Z.C.); and by the Foundational Questions Institute (fqxi.org; Grant No. FQXi-RFP-1617) through their fund at the Silicon Valley Community Foundation (R.M.N.).

[1] Y. Shimizu, K. Miyagawa, K. Kanoda, M. Maesato, and G. Saito, Spin Liquid State in an Organic Mott Insulator with Triangular Lattice, Phys. Rev. Lett. **91**, 107001 (2003).

[2] J. S. Helton, K. Matan, M. P. Shores, E. A. Nytko, B. M. Bartlett, Y. Yoshida, Y. Takano, A. Suslov, Y. Qiu, J.-H. Chung, D. G. Nocera, and Y. S. Lee, Spin Dynamics of the Spin-1/2 Kagome Lattice Antiferromagnet $ZnCu_3(OH)_6Cl_2$, Phys. Rev. Lett. **98**, 107204 (2007).

[3] T.-H. Han, J. S. Helton, S. Chu, D. G. Nocera, J. A. Rodriguez-Rivera, C. Broholm, and Y. S. Lee, Fractionalized excitations in the spin liquid state of a kagome lattice antiferromagnet, Nature (London) **492**, 406 (2012).

[4] A. Banerjee *et al.*, Proximate Kitaev quantum spin liquid behavior in a honeycomb magnet, Nat. Mater. **15**, 733 (2016).
[5] C. Balz *et al.*, Physical realization of a quantum spin liquid based on a complex frustration mechanism, Nat. Phys. **12**, 942 (2016).
[6] L. Balents, Spin liquids in frustrated magnets, Nature (London) **464**, 199 (2010).
[7] L. Savary and L. Balents, Quantum spin liquids, Rep. Prog. Phys. **80**, 016502 (2017).
[8] Y. Zhou, K. Kanoda, and T.-K. Ng, Quantum spin liquid states, Rev. Mod. Phys. **89**, 025003 (2017).
[9] M. A. Levin and X.-G. Wen, String-net condensation: A physical mechanism for topological phases, Phys. Rev. B **71**, 045110 (2005).
[10] M. J. Harris, S. T. Bramwell, D. F. McMorrow, T. Zeiske, and K. W. Godfrey, Geometrical Frustration in the Ferromagnetic Pyrochlore $Ho_2Ti_2O_7$, Phys. Rev. Lett. **79**, 2554 (1997).
[11] J. S. Gardner, M. J. P. Gingras, and J. E. Greedan, Magnetic pyrochlore oxides, Rev. Mod. Phys. **82**, 53 (2010).
[12] C. Castelnovo, R. Moessner, and S. L. Sondhi, Spin ice, fractionalization, and topological order, Annu. Rev. Condens. Matter Phys. **3**, 35 (2012).
[13] M. J. P. Gingras and P. A. McClarty, Quantum spin ice: A search for gapless quantum spin liquids in pyrochlore magnets, Rep. Prog. Phys. **77**, 056501 (2014).
[14] Y. Tokiwa *et al.*, Discovery of emergent photon and monopoles in a quantum spin liquid, J. Phys. Soc. Jpn. **87**, 064702 (2018).
[15] N. Martin, P. Bonville, E. Lhotel, S. Guitteny, A. Wildes, C. Decorse, M. Ciomaga Hatnean, G. Balakrishnan, I. Mirebeau, and S. Petit, Disorder and Quantum Spin Ice, Phys. Rev. X **7**, 041028 (2017).
[16] J.-J. Wen, S. M. Koohpayeh, K. A. Ross, B. A. Trump, T. M. McQueen, K. Kimura, S. Nakatsuji, Y. Qiu, D. M. Pajerowski, J. R. D. Copley, and C. L. Broholm, Disordered Route to the Coulomb Quantum Spin Liquid: Random Transverse Fields on Spin Ice in $Pr_2Zr_2O_7$, Phys. Rev. Lett. **118**, 107206 (2017).
[17] C. L. Henley, Power-law spin correlations in pyrochlore antiferromagnets, Phys. Rev. B **71**, 014424 (2005).
[18] C. L. Henley, The "Coulomb phase" in frustrated systems, Annu. Rev. Condens. Matter Phys. **1**, 179 (2010).
[19] T. Fennell, P. P. Deen, A. R. Wildes, K. Schmalzl, D. Prabhakaran, A. T. Boothroyd, R. J. Aldus, D. F. McMorrow, and S. T. Bramwell, Magnetic Coulomb phase in the spin ice $Ho_2Ti_2O_7$, Science **326**, 415 (2009).
[20] S. T. Bramwell, M. J. Harris, B. C. den Hertog, M. J. P. Gingras, J. S. Gardner, D. F. McMorrow, A. R. Wildes, A. L. Cornelius, J. D. M. Champion, R. G. Melko, and T. Fennell, Spin Correlations in $Ho_2Ti_2O_7$: A Dipolar Spin Ice System, Phys. Rev. Lett. **87**, 047205 (2001).
[21] A. Banerjee, J. Yan, J. Knolle, C. A. Bridges, M. B. Stone, M. D. Lumsden, D. G. Mandrus, D. A. Tennant, R. Moessner, and S. E. Nagler, Neutron scattering in the proximate quantum spin liquid α-$RuCl_3$, Science **356**, 1055 (2017).
[22] O. I. Motrunich and T. Senthil, Exotic Order in Simple Models of Bosonic Systems, Phys. Rev. Lett. **89**, 277004 (2002).
[23] R. Moessner and S. L. Sondhi, Three dimensional resonating valence bond liquids and their excitations, Phys. Rev. B **68**, 184512 (2003).
[24] M. Hermele, M. P. A. Fisher, and L. Balents, Pyrochlore photons: The $U(1)$ spin liquid in a $S = 1/2$ three-dimensional frustrated magnet, Phys. Rev. B **69**, 064404 (2004).
[25] O. I. Motrunich and T. Senthil, On the origin of artificial electrodynamics and other stories in three-dimensional bosonic models, Phys. Rev. B **71**, 125102 (2005).
[26] M. Levin and X.-G. Wen, Quantum ether: Photons and electrons from a rotor model, Phys. Rev. B **73**, 035122 (2006).
[27] B. Canals and D. A. Garanin, Classical spin liquid: Exact solution for the infinite-component antiferromagnetic model on the kagomé lattice, Phys. Rev. B **59**, 443 (1999).
[28] B. Canals and D. A. Garanin, Spin-liquid phase in the pyrochlore anti-ferromagnet, Can. J. Phys. **79**, 1323 (2001).
[29] A. Banerjee, S. V. Isakov, K. Damle, and Y. B. Kim, Unusual Liquid State of Hard-Core Bosons on the Pyrochlore Lattice, Phys. Rev. Lett. **100**, 047208 (2008).
[30] K. A. Ross, L. Savary, B. D. Gaulin, and L. Balents, Quantum Excitations in Quantum Spin Ice, Phys. Rev. X **1**, 021002 (2011).
[31] L. Savary and L. Balents, Coulombic Quantum Liquids in Spin-1/2 Pyrochlores, Phys. Rev. Lett. **108**, 037202 (2012).
[32] L. Savary and L. Balents, Spin liquid regimes at nonzero temperature in quantum spin ice, Phys. Rev. B **87**, 205130 (2013).
[33] C. Wang and T. Senthil, Time-Reversal Symmetric $U(1)$ Quantum Spin Liquids, Phys. Rev. X **6**, 011034 (2016).
[34] L. Savary, X. Wang, H.-Y. Kee, Y. B. Kim, Y. Yu, and G. Chen, Quantum spin ice on the breathing pyrochlore lattice, Phys. Rev. B **94**, 075146 (2016).
[35] L. Savary and L. Balents, Disorder-Induced Quantum Spin Liquid in Spin Ice Pyrochlores, Phys. Rev. Lett. **118**, 087203 (2017).
[36] L. Zou, C. Wang, and T. Senthil, Symmetry enriched $U(1)$ quantum spin liquids, Phys. Rev. B **97**, 195126 (2018).
[37] L. Zou, Bulk characterization of topological crystalline insulators: Stability under interactions and relations to symmetry enriched $U(1)$ quantum spin liquids, Phys. Rev. B **97**, 045130 (2018).
[38] C. Xu, Gapless bosonic excitation without symmetry breaking: Novel algebraic spin liquid with soft gravitons, Phys. Rev. B **74**, 224433 (2006).
[39] A. Rasmussen, Y.-Z. You, and C. Xu, Stable gapless Bose liquid phases without any symmetry, arXiv:1601.08235.
[40] M. Pretko, Subdimensional particle structure of higher rank U(1) spin liquids, Phys. Rev. B **95**, 115139 (2017).
[41] M. Pretko, Generalized electromagnetism of subdimensional particles, Phys. Rev. B **96**, 035119 (2017).
[42] P. Orland, Instantons and disorder in antisymmetric tensor gauge fields, Nucl. Phys. B **205**, 107 (1982).
[43] R. Pearson, Phase structure of antisymmetric tensor gauge fields, Phys. Rev. D **26**, 2013 (1982).
[44] S.-J. Rey, Higgs mechanism for Kalb-Ramond gauge field, Phys. Rev. D **40**, 3396 (1989).
[45] A. Lipstein and R. Reid-Edwards, Lattice gerbe theory, J. High Energy Phys. 09 (2014) 034.
[46] E. Lake, Higher-form symmetries and spontaneous symmetry breaking, arXiv:1802.07747.
[47] R. M. Nandkishore and M. Hermele, Fractons, arXiv:1803.11196.

[48] C. Chamon, Quantum Glassiness in Strongly Correlated Clean Systems: An Example of Topological Overprotection, Phys. Rev. Lett. **94**, 040402 (2005).
[49] S. Bravyi, B. Leemhuis, and B. M. Terhal, Topological order in an exactly solvable 3D spin model, Ann. Phys. **326**, 839 (2010).
[50] J. Haah, Local stabilizer codes in three dimensions without string logical operators, Phys. Rev. A **83**, 042330 (2011).
[51] C. Castelnovo and C. Chamon, Topological quantum glassiness, Philos. Mag. **92**, 304, (2012).
[52] B. Yoshida, Exotic topological order in fractal spin liquids, Phys. Rev. B **88**, 125122 (2013).
[53] S. Bravyi and J. Haah, Quantum Self-Correction in the 3D Cubic Code Model, Phys. Rev. Lett. **111**, 200501 (2013).
[54] S. Vijay, J. Haah, and L. Fu, A new kind of topological quantum order: A dimensional hierarchy of quasiparticles built from stationary excitations, Phys. Rev. B **92**, 235136 (2015).
[55] S. Vijay, J. Haah, and L. Fu, Fracton topological order, generalized lattice gauge theory and duality, Phys. Rev. B **94**, 235157 (2016).
[56] A. Prem, M. Pretko, and R. Nandkishore, Emergent phases of fractonic matter, Phys. Rev. B **97**, 085116 (2018).
[57] A. Prem, J. Haah, and R. Nandkishore, Glassy quantum dynamics in translation invariant fracton models, Phys. Rev. B **95**, 155133 (2017).
[58] D. J. Williamson, Fractal symmetries: Ungauging the cubic code, Phys. Rev. B **94**, 155128 (2016).
[59] S. Vijay, Isotropic layer construction and phase diagram for fracton topological phases, arXiv:1701.00762.
[60] H. Ma, E. Lake, X. Chen, and M. Hermele, Fracton topological order via coupled layers, Phys. Rev. B **95**, 245126 (2017).
[61] T. H. Hsieh and G. B. Halász, Fractons from partons, Phys. Rev. B **96**, 165105 (2017).
[62] K. Slagle and Y. B. Kim, Fracton topological order from nearest-neighbor two-spin interactions and dualities, Phys. Rev. B **96**, 165106 (2017).
[63] B. Shi and Y.-M. Lu, Deciphering the nonlocal entanglement entropy of fracton topological orders, Phys. Rev. B **97**, 144106 (2018).
[64] S. Vijay and L. Fu, A generalization of non-abelian anyons in three dimensions, arXiv:1706.07070.
[65] G. B. Halász, T. H. Hsieh, and L. Balents, Fracton Topological Phases from Strongly Coupled Spin Chains, Phys. Rev. Lett. **119**, 257202 (2017).
[66] K. Slagle and Y. B. Kim, Quantum field theory of X-cube fracton topological order and robust degeneracy from geometry, Phys. Rev. B **96**, 195139 (2017).
[67] V. V. Albert, S. Pascazio, and M. H. Devoret, General phase spaces: From discrete variables to rotor and continuum limits, J. Phys. A: Math. Theor. **50**, 504002 (2017).
[68] T. Devakul, S. A. Parameswaran, and S. L. Sondhi, Correlation function diagnostics for type-I fracton phases, Phys. Rev. B **97**, 041110 (2018).
[69] O. Petrova and N. Regnault, A simple anisotropic three-dimensional quantum spin liquid with fracton topological order, Phys. Rev. B **96**, 224429 (2017).
[70] H. Ma, A. T. Schmitz, S. A. Parameswaran, M. Hermele, and R. M. Nandkishore, Topological entanglement entropy of fracton stabilizer codes, Phys. Rev. B **97**, 125101 (2018).
[71] H. He, Y. Zheng, B. A. Bernevig, and N. Regnault, Entanglement entropy from tensor network states for stabilizer codes, Phys. Rev. B **97**, 125102 (2018).
[72] A. T. Schmitz, H. Ma, R. M. Nandkishore, and S. A. Parameswaran, Recoverable information and emergent conservation laws in fracton stabilizer codes, Phys. Rev. B **97**, 134426 (2018).
[73] K. Slagle and Y. B. Kim, X-cube fracton model on generic lattices: Phases and geometric order, Phys. Rev. B **97**, 165106 (2018).
[74] W. Shirley, K. Slagle, Z. Wang, and X. Chen, Fracton Models on General Three-Dimensional Manifolds, Phys. Rev. X **8**, 031051 (2018).
[75] T. Devakul, $\mathbb{Z}_3$ topological order in face-centered cubic quantum plaquette model, Phys. Rev. B **97**, 155111 (2018).
[76] M. Pretko and L. Radzihovsky, Fracton-Elasticity Duality, Phys. Rev. Lett. **120**, 195301 (2018).
[77] A. Gromov, Fractional topological elasticity and fracton order, arXiv:1712.06600.
[78] S. Pai and M. Pretko, Fractonic line excitations: An inroad from 3d elasticity theory, Phys. Rev. B **97**, 235102 (2018).
[79] H. Ma, M. Hermele, and X. Chen, Fracton topological order from Higgs and partial confinement mechanisms of rank-two gauge theory, Phys. Rev. B **98**, 035111 (2018).
[80] D. Bulmash and M. Barkeshli, The Higgs mechanism in higher-rank symmetric $U(1)$ gauge theories, Phys. Rev. B **97**, 235112 (2018).
[81] Y. You, T. Devakul, F. J. Burnell, and S. L. Sondhi, Subsystem symmetry protected topological order, Phys. Rev. B **98**, 035112 (2018).
[82] H. Ma and M. Pretko, Higher rank deconfined quantum criticality and the exciton Bose condensate, Phys. Rev. B **98**, 125105 (2018).
[83] W. Shirley, K. Slagle, and X. Chen, Universal entanglement signatures of foliated fracton phases, arXiv:1803.10426.
[84] A. Kubica and B. Yoshida, Ungauging quantum error-correcting codes, arXiv:1805.01836.
[85] T. Devakul, Y. You, F. J. Burnell, and S. L. Sondhi, Fractal symmetric phases of matter, arXiv:1805.04097.
[86] H. Song, A. Prem, S.-J. Huang, and M. A. Martin-Delgado, Twisted fracton models in three dimensions, arXiv:1805.06899.
[87] Y. You, T. Devakul, F. J. Burnell, and S. L. Sondhi, Symmetric fracton matter: Twisted and enriched, arXiv:1805.09800.
[88] D. Bulmash and M. Barkeshli, Generalized $U(1)$ Gauge field theories and fractal dynamics, arXiv:1806.01855.
[89] O. Benton, L. D. C. Jaubert, H. Yan, and N. Shannon, A spin liquid with pinch-line singularities on the pyrochlore lattice, Nat. Commun. **7**, 11572 (2016).
[90] P. H. Conlon and J. T. Chalker, Spin Dynamics in Pyrochlore Heisenberg Antiferromagnets, Phys. Rev. Lett. **102**, 237206 (2009).
[91] J. Robert, B. Canals, V. Simonet, and R. Ballou, Propagation and Ghosts in the Classical Kagome Antiferromagnet, Phys. Rev. Lett. **101**, 117207 (2008).
[92] A. Prem, S. Vijay, Y.-Z. Chou, M. Pretko, and R. Nandkishore (unpublished).